

UNCLASSIFIED

AD 4 6 1 2 6 7

DEFENSE DOCUMENTATION CENTER

FOR

SCIENTIFIC AND TECHNICAL INFORMATION

CAMERON STATION ALEXANDRIA, VIRGINIA



UNCLASSIFIED

NOTICE: When government or other drawings, specifications or other data are used for any purpose other than in connection with a definitely related government procurement operation, the U. S. Government thereby incurs no responsibility, nor any obligation whatsoever; and the fact that the Government may have formulated, furnished, or in any way supplied the said drawings, specifications, or other data is not to be regarded by implication or otherwise as in any manner licensing the holder or any other person or corporation, or conveying any rights or permission to manufacture, use or sell any patented invention that may in any way be related thereto.

461267

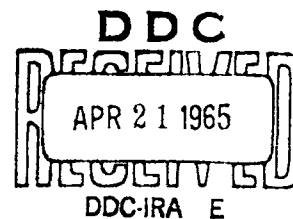
CATALOGED BY: DDC 461267
AS AD 110

ATL-TR-65-26

ATTENUATION OF SHOCKS PRODUCED BY UNLIKE METAL IMPACT

by
J. F. Heyda, T. D. Riney, Gen Elec Co.

APRIL 1965



Directorate of Armament Development
Det 4, Research and Technology Division
Air Force Systems Command
Eglin Air Force Base, Florida

Qualified users may obtain copies of this report from the Defense Documentation Center.

Do not return this copy. Retain or destroy.

ATTENUATION OF SHOCKS PRODUCED BY UNLIKE METAL IMPACT

By
J. F. Heyda, T. D. Riney, Gen Elec Co.

FOREWORD

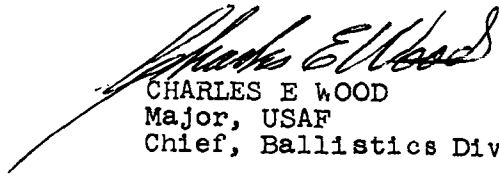
This interim report was prepared by the Mechanics Section of the Space Sciences Laboratory of the General Electric Company's Missile and Space Division, under Air Force Contract AF08(635)-3781, "Theoretical Terminal Ballistic Study; Energy Dissipation During Impact." The work was administered under the direction of the Terminal Ballistics Branch, Det. 4, Research and Technology Division, Eglin Air Force Base with Mr. A. G. Bilek and Lt. M. S. Harris as Project Engineers.

The major part of the work during the last six months has been directed towards the improvement of the computer codes for the solution of hyper-velocity impact problems. This work is only briefly described here, but the authors wish to acknowledge the contributions of Mr. T. Coffin, and Mrs. J. Goldman in this effort. They are also indebted to Mr. O. A. Winter for assistance in the calculations with the analytical model.

Publication of this report does not constitute Air Force approval of the report's findings or conclusions. It is published only for the exchange and stimulation of ideas.

PUBLICATION REVIEW

This technical report has been reviewed and is approved.



CHARLES E WOOD
Major, USAF
Chief, Ballistics Division

ABSTRACT

An analytical model is presented for determining the peak axial pressure generated at various depths in the target when impacted at hypervelocity by a projectile of similar or dissimilar material. Detailed calculations are given for impact of aluminum, iron, lead and copper into aluminum targets. Available experimental data for impact into aluminum targets are discussed in terms of the theory.

TABLE OF CONTENTS

Section	Page
I. Introduction	1
II. Codes and Computer Facilities	3
III. Review and Formulation of Analytical Model	4
IV. Extension of the Model to Dissimilar Materials	10
V. Relation to Other Investigations	15
VI. Conclusions	19
References	20

LIST OF SYMBOLS

t	time variable
p	pressure
ρ	density of medium
ρ_o	undisturbed density
x	compression ratio $(= \rho_o / \rho)$
L	radius of cylindrical projectile
l	length of cylindrical projectile
\bar{L}	characteristic length $(= \sqrt[3]{L^2 l})$
D_s	diameter of equi-volume sphere
P_c	penetration depth of crater
C	coefficient in penetration formula
v_o	impact velocity
v_o^*	threshold value for energy scaling
E_o^*	threshold energy for energy scaling
$()_H$	subscript denoting value on the Hugoniot
δ	ratio of projectile density to target density $(= \rho_p / \rho_t)$
R	distance below target surface of shock
\dot{R}	shock velocity in target
c_H	sound velocity in shocked material
A, K, R_o	parameters in analytical model
R_1	position where shock in target first attenuated on axis

SECTION I

INTRODUCTION

In two earlier interim reports [1, 2] numerical calculations were presented describing the time dependent flow field produced when a projectile impacts a target at hypervelocity. The calculations were made using a computer code (PICWICK I) for solving the complex system of equations governing a visco-plastic model of the process. The results indicated that in a thick target the depth of penetration, of geometrically similar projectiles of like metal, varies with the impact velocity according to $v_o^{2/3}$ in the hypervelocity regime. Calculations were also given to show that the crater dimensions are relatively insensitive to the density of homogeneous projectiles of the same basic material. Experimentally observed size effects were discussed in terms of the visco-plastic model and it was concluded that the threshold velocity for energy scaling will depend somewhat on the dimensions of the projectile.

The formula for the depth of penetration based on these results is as follows:

$$P_c = C(\rho_p / \rho_t)^{1/3} v_o^{2/3} (v_o \geq v_o^*, E_o \geq E_o^*), \quad (1)$$

where the constants C , v_o^* and E_o^* must be experimentally determined. E_o^* is a threshold impact energy which reflects the size effect on the threshold impact velocity v_o^* . The material parameters are known from experiment to vary among alloys of nominally the same metal, reflecting strength and strain-rate effects that in the late stages of the flow process determine the final crater dimensions.

Plate targets of finite thickness were also studied in the earlier reports. The forward momentum carried by the spallation bubble from the rear surface of the target was computed for two plate thicknesses. The spatial divergence of the bubble and the corresponding decrease in its projected momentum density was charted. The spread of the loading and the maximum value of the projected momentum density was obtained as a function of the standoff distances. These results are useful in analyzing meteor bumper protection systems. Preliminary calculations were also presented for impact into a target consisting of two spaced plates.

Many important and unresolved questions remain to be studied, especially for finite plate targets and meteor bumper systems. Other problems of practical interest are the penetration effectiveness of projectiles of special geometry. An improved version of the code (PICWICK II) has been under development to treat these problems. Some recently added features are briefly described in the first part of this report. Up to this time, however, computer time has not been available to utilize the improved capability of the code in production runs. The IBM 7094 at Eglin AFB, used for the earlier calculations, has been used to capacity on higher priority projects.

A recently developed analytical description [3] of the amplitude and velocity of the shock wave produced in a target under end-on impact by a like-metal cylindrical projectile is summarized in this report. The analysis is then extended to provide the peak axial pressure generated at various depths in the target when the projectile and target materials are different. Detailed results are given for impact of aluminum, iron, lead, and copper into aluminum targets.

Finally, a summary of experimental data for impact of aluminum, steel, tungsten, and glass projectiles into aluminum targets is given and the results are discussed in terms of the theory.

SECTION II

CODES AND COMPUTER FACILITIES

In developing PICWICK II the same basic numerical scheme was used as in PICWICK I, but magnetic tapes are employed as external storage to permit a four-fold increase in the number of cells in the computational mesh. The code now permits approximately a 2000 cell mesh when using the full visco-plastic model. The code is presently operational in Fortran 2 as a Chain Job and in Fortran 4 as an Overlay. These two methods of sharing internal storage were employed so that repartitioning of the mesh could be accomplished with a minimum of the memory capacity of the IBM 7094. The repartitioning process allows a doubling of the linear dimensions of the cells in the computational mesh at desired stages of the cratering process to permit a greater volume of the target to be studied by the same number of cells. Thus the disturbance described by four cells at the instant prior to repartitioning is described by a single cell immediately subsequent.

The four-fold increase in the number of cells in the mesh provided by PICWICK II would normally mean a comparable increase in the computer time required for each cycle of the calculations. It has proved possible, however, to reduce the calculation time that would otherwise be required for an impact problem by about one-third. A Bypass subroutine has been incorporated which avoids making calculations in that part of the finite-difference mesh as yet undisturbed by the flow process. This device is especially effective in the early stages of the flow and after each repartitioning process.

Unfortunately computer time on the IBM 7094 at Eglin has not been available to utilize the new capabilities of the code. However, provisions have recently been made to use an alternate Air Force facility. More detailed studies of meteor bumper systems will be made. Impact by hollow cylindrical projectiles will also be treated.

SECTION III

REVIEW AND FORMULATION OF ANALYTICAL MODEL

In reference [3] it was shown that for end-on hypervelocity impact of a solid right-circular cylinder into a semi-infinite medium of like material the peak axial pressure in the target, its position and speed of propagation, can be determined accurately from an analytical model. This model assumes that the axial shock front, immediately after impact, moves with the constant impact shock speed R_H until the point R_1 is reached where the axial shock is first attenuated by rarefaction waves arising at impact at the projectile edge. This attenuation manifests itself by a rapid release of energy over a short axial distance, the effect approximating a line blast. At the very beginning of this period the shock front is planar and moving with the speed of a planar blast wave; however, the line blast effect diminishes the planar blast wave speed by an amount that is proportional to the speed of the cylindrically radial blast wave generated by it. As shown in more detail in reference [3] the pressure pulse moves into the target along the axial direction so that its position R , measured from the point of impact, satisfies the differential equation

$$\dot{R} = A \left[\frac{4k}{\sqrt{R-R_0}} - \frac{4k^2}{R-R_0} \right], \quad (2)$$

where A , k , R_0 are parameters of the motion and it is understood that (2) is valid for $R \geq R_1$. For $0 \leq R \leq R_1$, as mentioned above, we have $\dot{R} = R_H$ where R_H is determined from the one-dimensional impact of two semi-infinite bodies, the corresponding impact interface pressure being denoted by p_H . The parameter k^2 has dimensions of a length and can be regarded as a measure of the average distance over which the line blast effect is operative. We shall find it more convenient, however, to non-dimensionalize this parameter and use instead the parameter

$$K = \frac{k}{\sqrt{L}}, \quad \bar{L} \equiv (L^2 \ell)^{1/3} = L \left(\frac{\ell}{L} \right)^{1/3} \quad (3)$$

where L , ℓ are, respectively, the projectile radius and length.

The peak axial pressure profile can now be computed as a function of R from the following simultaneous set of three equations:

$$\frac{R}{\bar{L}} = \frac{R_0}{\bar{L}} + \left[\frac{2K}{1 - \sqrt{1 - \frac{\dot{R}}{A}}} \right]^2 \quad (4)$$

$$\dot{R} = \sqrt{\frac{p(x)}{\rho_0 (1-x)}} \quad (5)$$

$$p = p(x), \quad x \equiv \rho_0 / \rho \quad (6)$$

where (4) is (2) in non-dimensional form and R_0/\bar{L} is given by

$$\frac{R_0}{\bar{L}} = \frac{R_1}{\bar{L}} - \left[\frac{2K}{1 - \sqrt{1 - \frac{\dot{R}_H}{A}}} \right]^2 \quad (7)$$

Equation (5) is a combination of two of the Rankine-Hugoniot jump relations valid across the shock, while equation (6) is the Hugoniot equation of state of the target medium. The variable ρ is taken as the density behind the shock. The energy release point R_1 appearing in (7) is computed from the formula

$$R_1 = L \dot{R}_H / [c_H^2 - x_H^2 \dot{R}_H^2]^{1/2}, \quad (8)$$

where x_H is the impact value of x and c_H is the impact value of the hydrodynamic sound speed, namely

$$c_H^2 = -x_H^2 \left[\left(\frac{dp}{dx} \right)_{x=x_H} \right] / \rho_0 \quad (9)$$

The pressure profile for $R \geq R_1$ is conveniently plotted by letting x be the running variable, taking it in the interval $x_H \leq x \leq 1$. As x varies, R and p are determined and one then plots p vs R . The function $p(x)$ is normally quite involved and does not permit an explicit determination of its inverse.

To use equations (4, 5, 6) one must know the parameter values A , K and R_0 . The parameter A is determined by requiring the peak axial pressure profile to have a point of inflection at $R = R_1$. In actuality it has a corner there; little is lost, however, if one approximates the physical process by a continuous curve with a continuous slope. This assumption leads to an explicit determination of A in the form

$$A = \dot{R}_H f(\beta), \quad (10)$$

where

$$f(\beta) = \frac{51 - 44\beta + 8\beta^2 - 3\sqrt{33-8\beta}}{8(1-\beta)(4-\beta)}, \quad (11)$$

and β is in turn computed from the formulas

$$\beta = 4d_1 \left(1 - \frac{d_1}{d_2} \right) \quad (12)$$

$$d_1 = p_H / (p_H + [1 - x_H] p_H')$$

$$d_2 = 2p_H' / (1 - x_H) p_H''$$

where

$$p'_H \equiv (dp/dx)_{x=x_H}, \text{ etc.}$$

As v_o ranges over all hypervelocities of interest, the dimensionless quantity β varies from -1 to 0. The quantity $f(\beta)$, however, exhibits variation only in the third decimal place, being approximately equal to 1.055.

The parameter R_o is known once K is available since by substituting the data ($R = R_1$, $R = R_H$) into (4) we get relation (7).

The shock position R along the axis at time t since impact is obtained by solving the differential equation (2) and evaluating the constant of integration for conditions at the point R_1 . We find,

$$\begin{aligned} \frac{t}{L} = & \frac{R_1/\bar{L}}{\dot{R}_H} + \frac{1}{2AK} \left\{ \frac{1}{3} \left(\frac{R}{L} - \frac{R_o}{L} \right)^{3/2} + \frac{K}{2} \left(\frac{R}{L} - \frac{R_o}{L} \right) \right. \\ & + K^2 \sqrt{\frac{R}{L} - \frac{R_o}{L}} + K^3 \ln \left(\sqrt{\frac{R}{L} - \frac{R_o}{L}} - K \right) \\ & \left. - K^3 \left(\ln K + \frac{20}{3} \right) \right\}. \end{aligned} \quad (13)$$

In determining the all-important parameter K use was made of the PICWICK code solutions of the partial differential equations defining the hydrodynamic phase of the impact generated flow. In these solutions the projectile and target were of like material and the projectile shape was the standard one for which $L = \ell$. From a study of many such impact cases it was determined that K has the form

$$K = \alpha v_o^{-1/3}, \quad (14)$$

where α is a parameter characterizing the target material. In all these cases where $L = \ell$, we note that \bar{L} is also equal to L . For differently shaped projectiles; i. e., for those where $L \neq \ell$, eq. (14) may still be valid provided the aspect ratio ℓ/L does not differ from unity by a factor greater than about three. To test this hypothesis the form (14) was used for a case of lead-lead impact at $v_o = 1 \text{ cm}/\mu\text{sec}$ with $L = 1.8 \text{ cm}$ and $\ell = 3.6 \text{ cm}$, the shape factor here being $\sqrt{2}$. It was found that the (R, t) curve, using (13), matched the hydrodynamic code solutions for this case almost exactly (see Fig. 16 of [3]).*

*If k were made dimensionless by dividing L instead of \bar{L} then the form factor $(\ell/L)^{1/6}$ would have to appear in the associated parameter K .

The manner in which K should be modified when projectile and target are not of identical material was given a preliminary investigation by considering impacts of aluminum projectiles of differing bulk densities into aluminum. PICWICK solutions were obtained for $L = \ell$ shaped projectiles at speeds $v_0 = 0.76$ and $2.0 \text{ cm}/\mu\text{sec}$. A study of these solutions showed that the form of K given by (14) needed to be modified by a density factor, namely $1 + 0.15(1 - \delta)$, where $\delta = \rho_p/\rho_t$ is the ratio of the projectile density to the target density. The corresponding profiles matched the PICWICK profiles remarkably well, even with δ as low as $1/6$ (see the appropriate figures in reference 4). Since

$$1 + 0.15(1 - \delta) \doteq 1 + (\delta - 1)^{-1/6} \equiv \delta^{-1/6},$$

for δ close to 1, it is conjectured here that the appropriate density factor for the general case of dissimilar materials should be $\delta^{-1/6}$. The appropriate K would then be

$$K = \alpha v_0^{-1/3} \delta^{-1/6} \quad (15)$$

The analytical model and the PICWICK computations jointly confirm that a thick target sees no essential difference between the like-metal impacts of geometrically similar projectiles of equal kinetic energies. This is amply demonstrated in Figures 1, 2. Figure 1, which appeared as Figure 10 of reference 3, shows the peak axial pressure profiles generated by the impacts of two equi-energy aluminum projectiles into aluminum, one having dimensions $\ell = L = 0.26192 \text{ cm}^*$ and speed $v_0 = 2.0 \text{ cm}/\mu\text{sec}$; the other, larger and slower, with speed $v_0 = 0.76 \text{ cm}/\mu\text{sec}$ and dimensions $\ell' = L' = 0.49922$. The pressure curves have essentially coalesced into one at about 1.4 cm below the original target surface at a pressure of about 0.3 mb. There is, however, a difference in the times at which the pressure pulses for the two impacts pass a given axial location R . This is also shown in Figure 1, where it is seen that the pulse generated by the larger, slower projectile arrives at an axial location R some $0.35 \mu\text{sec}$ later than the arrival of the pulse generated by the smaller faster projectile. This time lag was observed in the PICWICK data and was discussed in earlier reports 1, 2.

Figure 2, taken from the work of reference 6, shows again the situation involving aluminum projectiles impacting aluminum; however, here we compare three projectile impacts, all at speed $v_0 = 2.0 \text{ cm}/\mu\text{sec}$, but involving projectiles of differing bulk densities (and hence, for equi-energy, of differing sizes). The projectiles are of normal density, density $1/3$ normal and density $1/6$ normal. Coalescence of the pressure profiles is obtained at a depth of approximately 0.8 cm below the target surface at a pressure of about 1 mb.

* These dimensions were selected so that the cylinder would have a volume equal to the volume of a $3/32$ " sphere. In this report the gram-centimeter-microsecond system of units is used throughout.

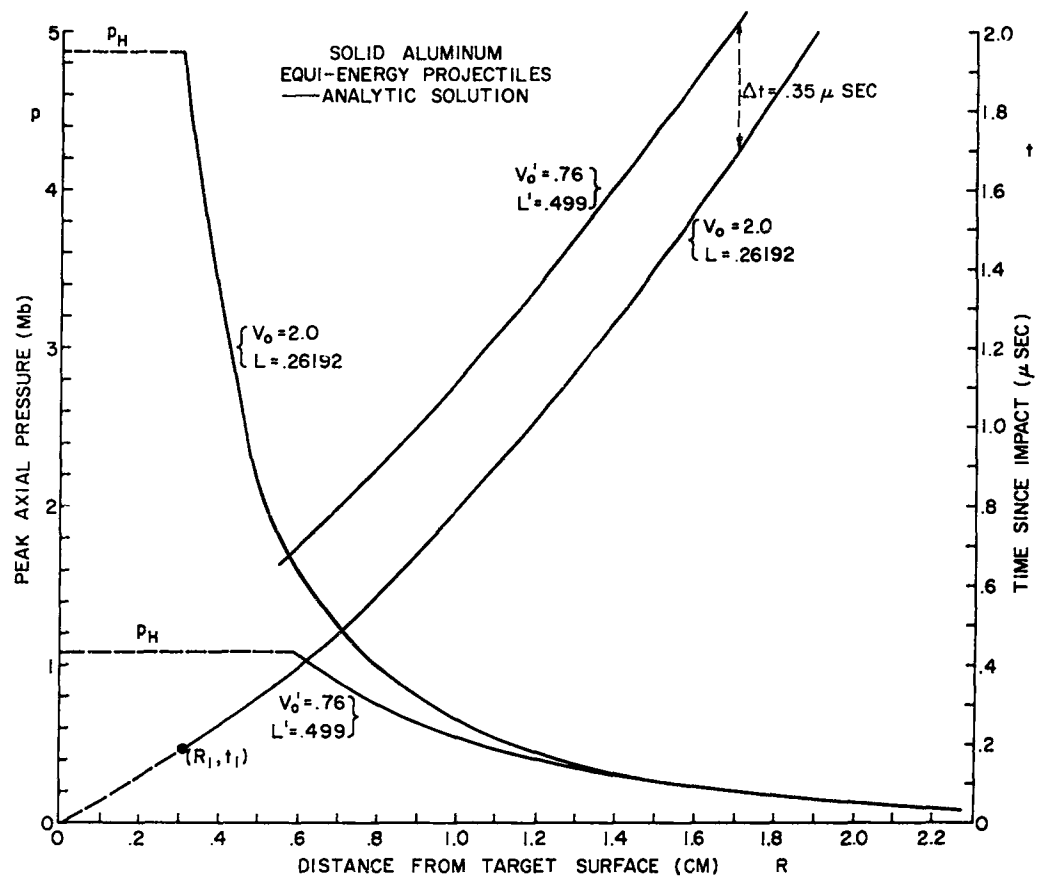


Figure 1. Comparison of shock waves produced in an aluminum target impacted by geometrically similar projectiles of aluminum. Analytic solutions are compared for impact velocities of .76 and 2.0 cm/μsec.

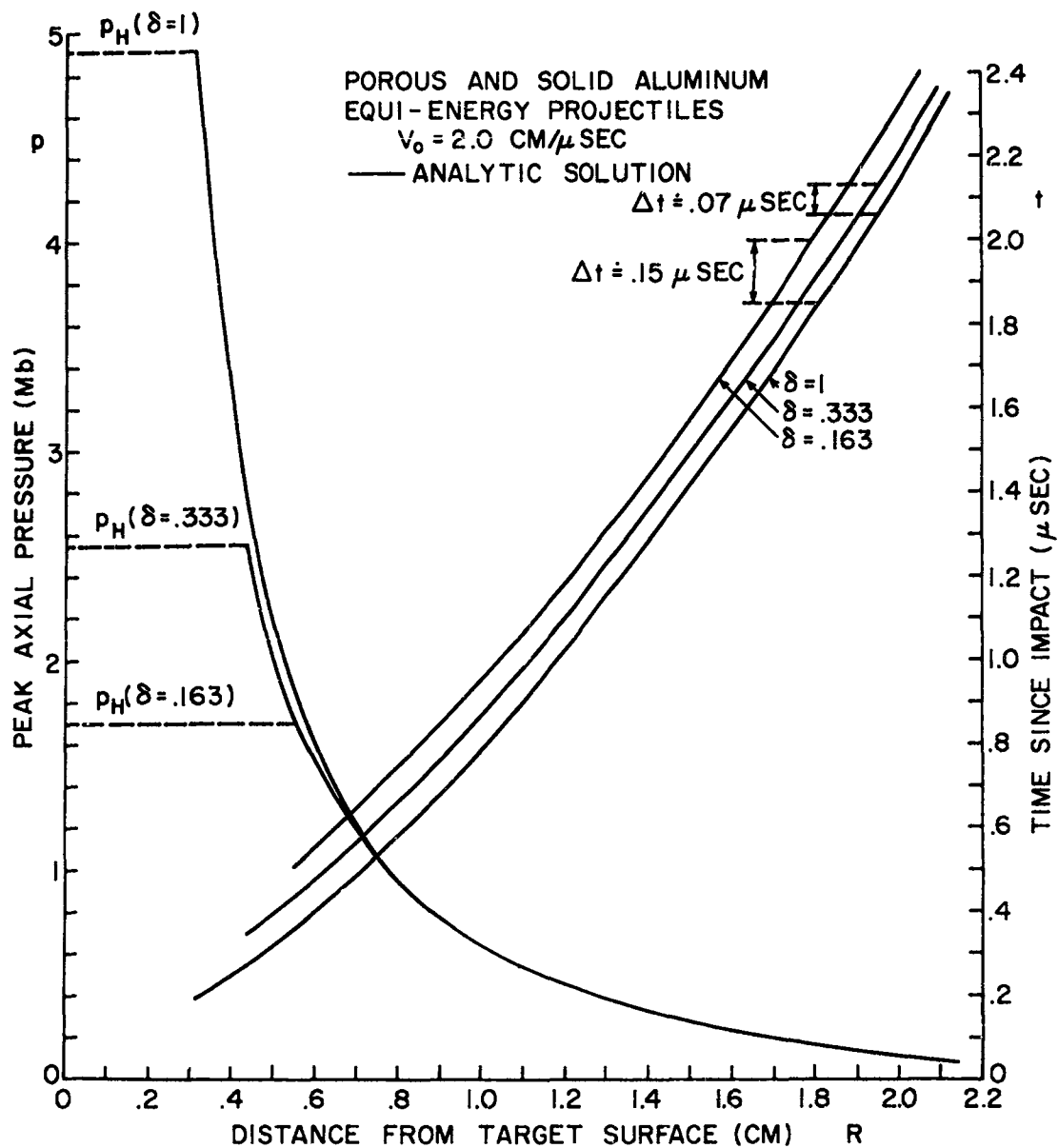


Figure 2. Comparison of shock waves produced in a solid aluminum target when impacted at $2.0 \text{ cm}/\mu \text{ sec}$ by normal and reduced density aluminum projectiles. Results depicted for $L = l = .26192$ ($\delta = 1$), $L = l = .3778$ ($\delta = .333$), and $L = l = .4797$ ($\delta = .163$).

SECTION IV

EXTENSION OF THE MODEL TO DISSIMILAR MATERIALS

When projectile and target are of dissimilar materials, the first step in determining the peak pressure profile is the evaluation of the necessary constants X_H , R_H , p_H , A and R_1 . This is greatly facilitated by use of the simple computer program described in [3] for computing Hugoniot values at impact. Their values depend on the impact velocity, the equations of state of impacting materials, and the geometry of the projectile.

The principal question involved in extending the analytical model to dissimilar projectile and target materials is what one should use for K . PICWICK solutions are presently not available for helping to decide this directly; however, one can lean on those PICWICK solutions involving target and projectile of like material but where the projectile has reduced bulk density (an approximation to porosity). In effect, then, one extrapolates the form of K given by (15) to be applicable to any two dissimilar materials. This form can be rewritten in the following interesting fashion:

$$K = \frac{\alpha^*}{(E_p/M_t)^{1/6}}, \quad (16)$$

where E_p is the kinetic energy of the projectile and M_t is a mass of target material having the same volume as that of the projectile. α^* is merely $\alpha/\sqrt{2}$ and so is again simply a numerical parameter characteristic of the target medium. Thus, K has a physical interpretation, being expressed in terms of the energy distribution produced in the target medium by the impacting projectile.

Computations were made using the analytical model and the extrapolated K given by (16) for impacts involving iron, copper, lead, and aluminum projectiles. The results are illustrated in Figures 3, 4, and 5.

In Figure 3, pressure profiles are shown for geometrically similar ($l = L$) equi-energy projectiles of iron, copper, lead, and aluminum impacting a thick aluminum target at $v_0 = 2.0 \text{ cm}/\mu\text{sec}$. The aluminum projectile has $L = 0.26192 \text{ cm}$; the other projectiles then have dimensions in accordance with energy scaling. These are given on the figure. The coalescence of the profiles is quite remarkable for the iron and copper. The iron, copper, and aluminum profiles all coalesce for pressures below 0.8 mb. The lead profile, however, remains distinct even at pressures less than 0.2 mb.

Figure 4 gives pressure profiles for three equi-energy aluminum projectiles at $v_0 = 2.0 \text{ cm}/\mu\text{sec}$ but with differing aspect ratios, namely $l/L = 2, 1$, and $1/2$. Again the pressure profiles tend to converge and very nearly coalesce but at pressures less than 0.2 mb.

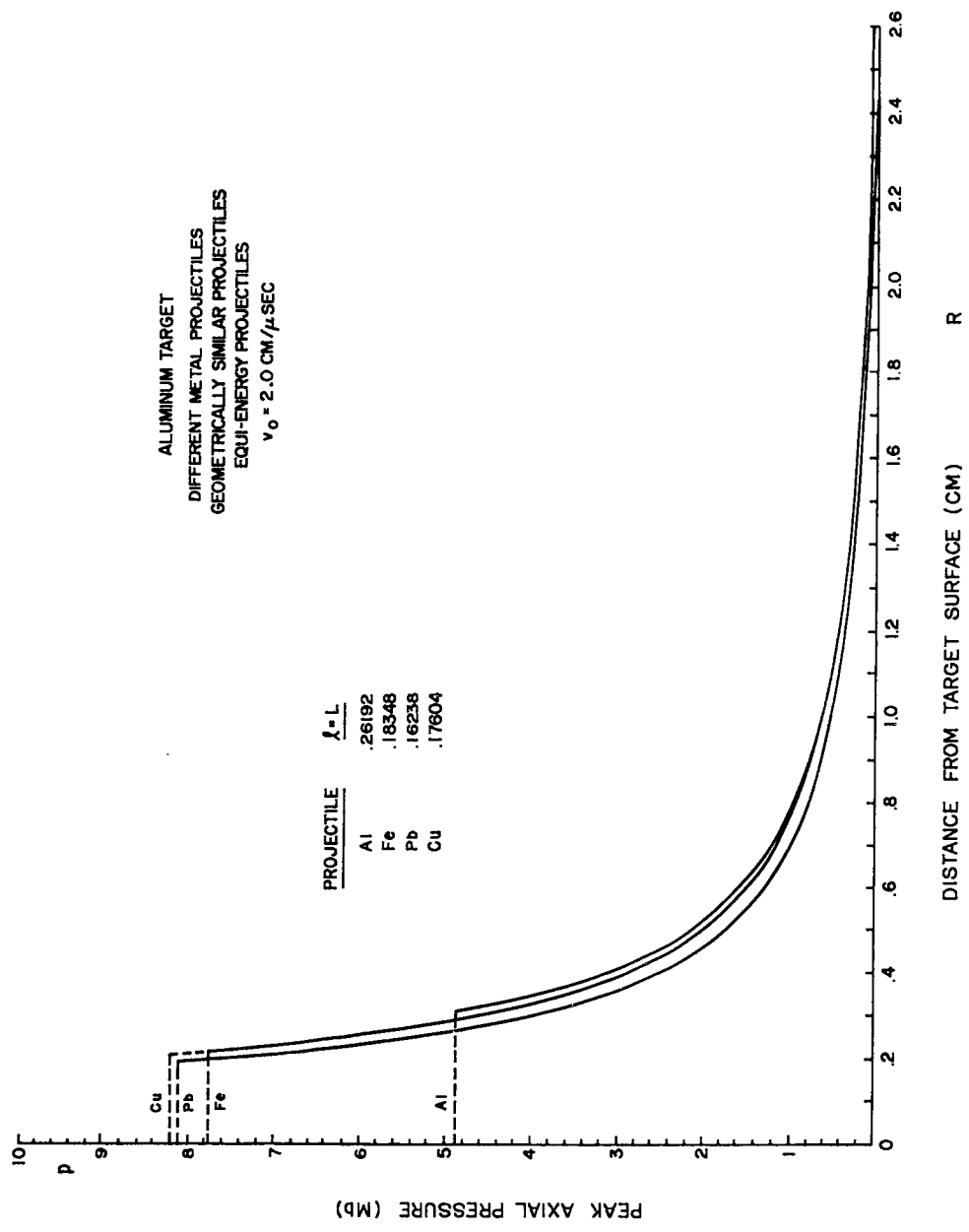


Figure 3. Peak pressures produced along the axis of an aluminum target impacted at 2.0 cm/ μ sec by geometrically similar, equi-mass projectiles of indicated metal.

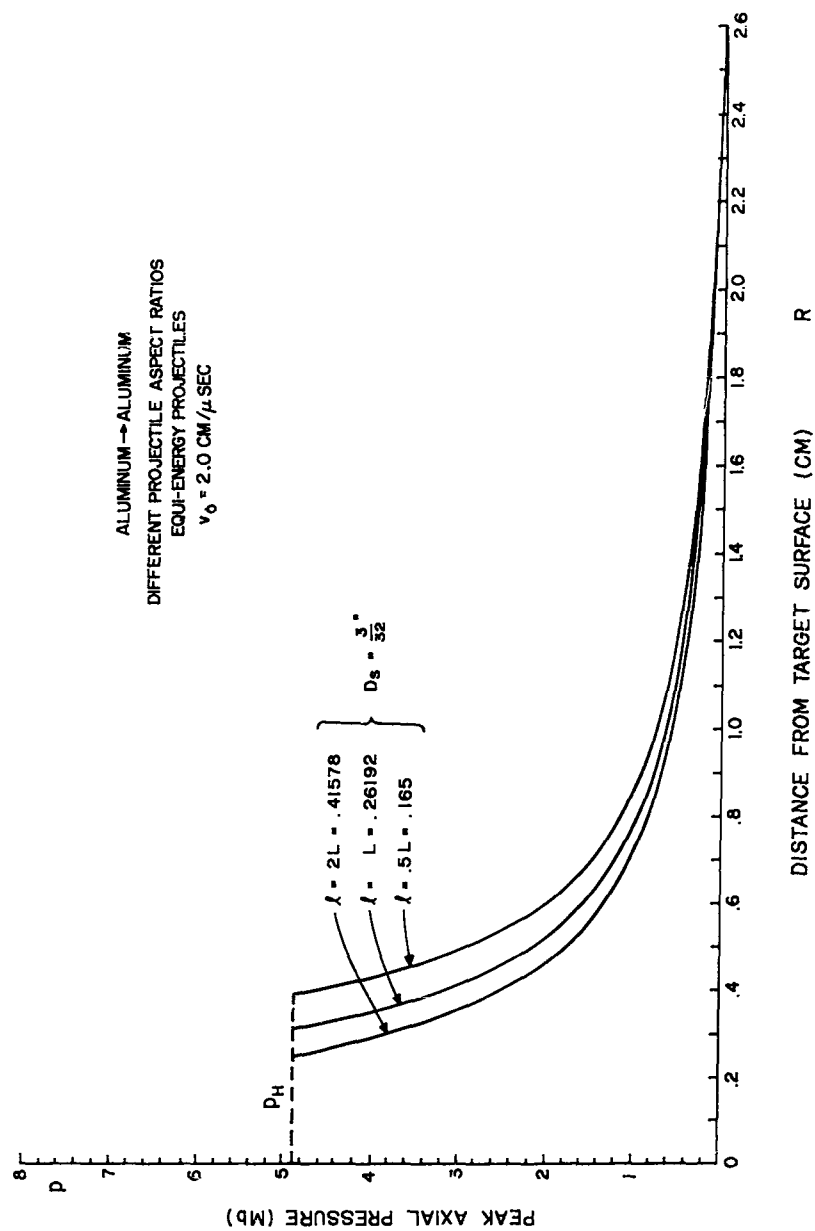


Figure 4. Peak pressures produced along the axis of an aluminum target impacted at $2.0 \text{ cm}/\mu \text{ sec}$ by equi-mass cylindrical aluminum projectiles of indicated aspect ratios.

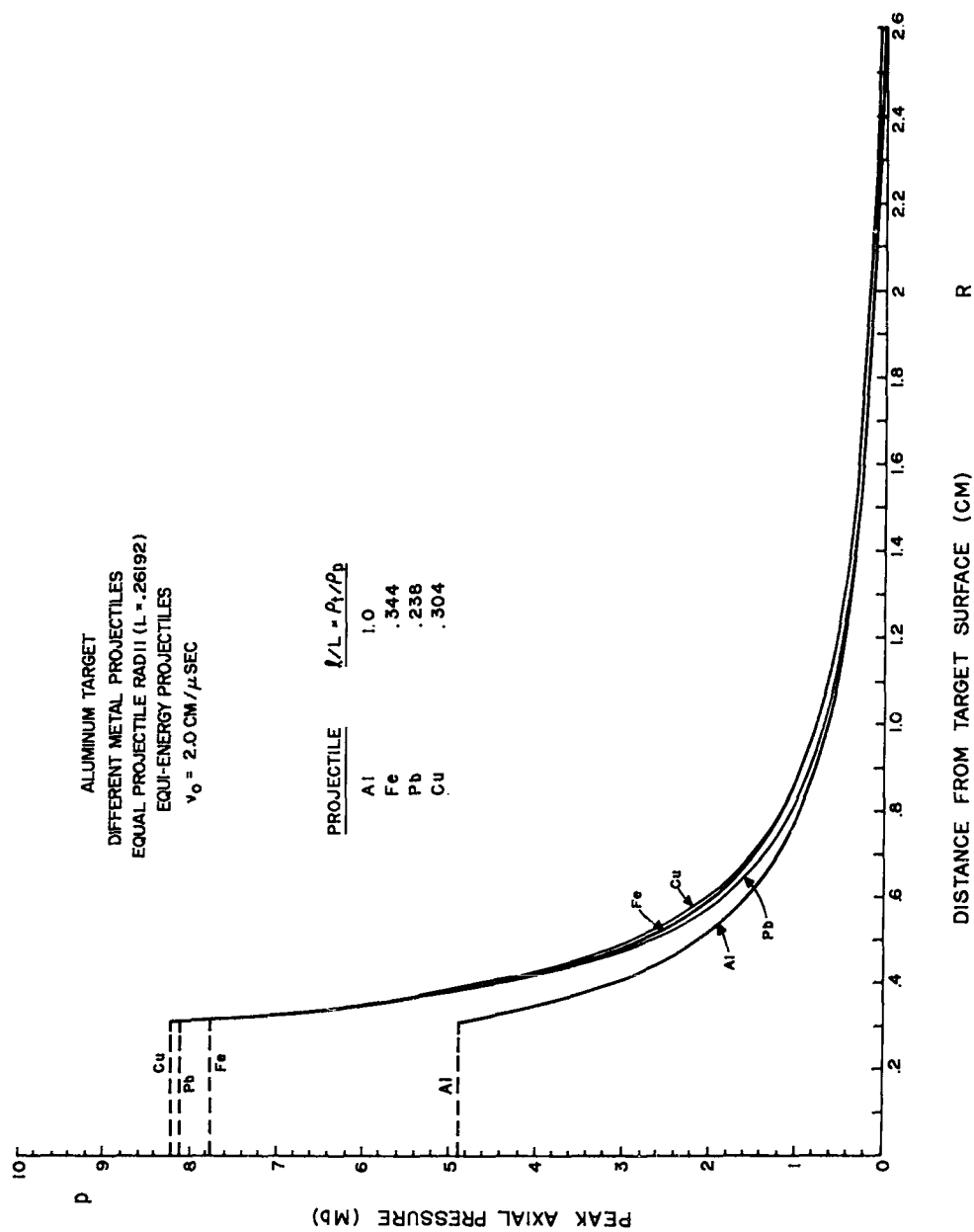


Figure 5. Peak axial pressures in an aluminum target impacted at $2.0 \text{ cm}/\mu\text{sec}$ by equi-mass cylindrical projectiles of indicated metals and aspect ratios.

Figure 5 shows the pressure profiles of iron, copper, lead and aluminum projectiles which are equi-energy (with $v_0 = 2.0 \text{ cm}/\mu\text{sec}$) but not geometrically similar. Using the aluminum projectile with $L = \ell = 0.26192 \text{ cm}$ as a standard the dimensions of the other projectiles p were computed from

$$\ell/L = \rho_{\text{Al}}/\rho_p.$$

Thus, all the projectiles have the same radius but differing lengths. Again the profiles tend to converge but do not completely coalesce even at pressures less than 0.2 mb.

SECTION V

RELATION TO OTHER INVESTIGATIONS

The peak axial pressure profiles calculated by the foregoing theory serve as valuable supplementary information to detailed numerical calculations. A characteristic of numerical solutions obtained with finite difference schemes is an oscillation of computed pressures about the true value. This is especially true of particle-in-cell type calculations as a consequence of the discrete nature of the mass representation. Yet only the detailed numerical calculations describe the complete flow field behind the shock front. It is the momentum content of this total disturbance produced in the target that determines the final impact damage.

Detailed hydrodynamic calculation for unlike metal impact have been reported by Walsh, et al [5]. They concluded that in the hypervelocity regime the material of the impacting projectile did not significantly affect the flow produced in the target. The projectile aspect ratio was also found to be insignificant provided it is within a factor of 3 of unity. These conclusions are actually incorporated into our extrapolations of the K in the analytical theory. The approximate merging of the pressure profiles depicted in Figures 3, 4, and 5 appear to be in general agreement with these conclusions. The coalescence, however, is not as unambiguous as for the impacts by geometrically similar equi-energy projectiles of like materials at different velocities (Figures 1 and 12) or of geometrically similar projectiles of reduced bulk density (Figure 2).

Several experimenters have studied the penetration of projectiles of various materials into thick aluminum (2024-Al) targets. Figure 6 is a composite plot depicting the crater depth as a function of impact velocity for aluminum, steel, tungsten, and borosilicate glass projectiles. It is interesting to discuss the data in terms of the theoretical studies.

The data for the aluminum and steel projectiles are seen to extend to above their respective threshold velocities for energy scaling. The data appear to be meshing into the indicated hatched regions bounded by lines of slope = 2/3. Now, if the cratering process were indeed independent of the projectile material, the constant C appearing in the penetration formula (1) would depend only on the target material. Consequently, at a given impact velocity $v_0 > v_0^*$, the following ratio would hold for the steel and aluminum projectiles impacting a target of given material,

$$\frac{(P_c/D_s)_{Fe-Al}}{(P_c/D_s)_{Al-Al}} = \left(\frac{\rho_{Fe}}{\rho_{Al}} \right)^{1/3} = 1.43$$

The centers of the hatched regions in the plots actually satisfy a ratio closer to 2.

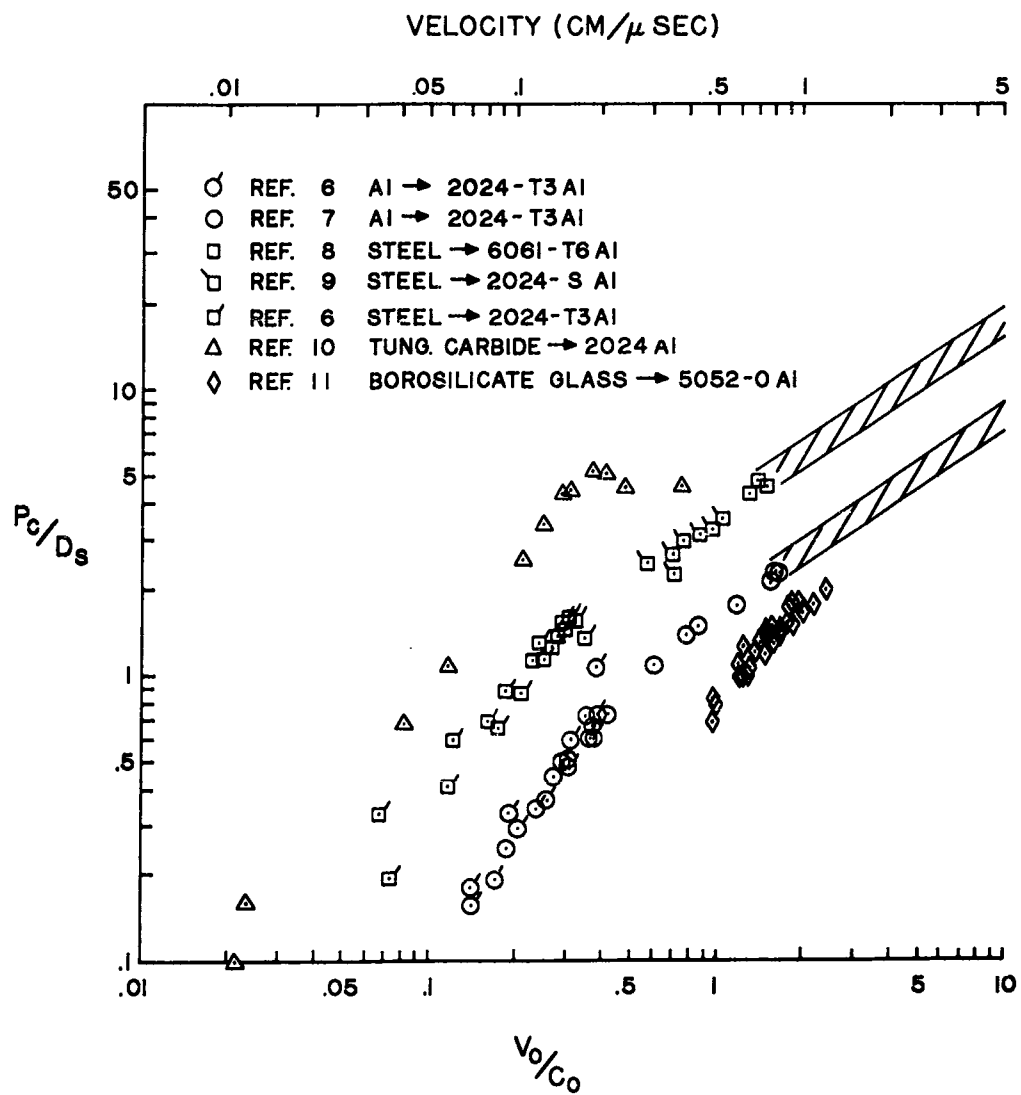


Figure 6. Experimental data depicting the depth of penetration at indicated impact velocity. This composite plot was made available by E. P. Bruce. P_c is the crater depth and D_s is the diameter of the projectile.

With these experimental facts in mind, further detailed calculations should be made to determine the momentum content of the deformation wave produced in a target by equi-energy projectiles of material different from that of the target.

The velocities attained in the tests with tungsten projectiles are considerably below the sound velocity in aluminum; the data are below the threshold velocity for energy scaling. The penetration increases nearly linearly with increased velocity until $v_o = .125 \text{ cm}/\mu \text{ sec}$. It then increases to a maximum before falling off slightly with increased velocity for velocities in the range .14 to .20 $\text{cm}/\mu \text{ sec}$. A similar phenomenon was also observed in studies of impact of tungsten spheres into lead [12]. There the critical velocity range of .05 to .08 $\text{cm}/\mu \text{ sec}$, was found to be associated with the fragmentation of the brittle tungsten projectile. At higher velocities the crater became hemispherical and the penetration increased in accordance with $v_o^{2/3}$. In Figure 7, the maximum pressure produced in a tungsten projectile impacting both lead and aluminum targets is shown as a function of impact velocity. It is seen that for both target materials and the critical impact velocities produced a pressure of about .11 to .33 mb in the projectile. It is predicted that, as was the case with impact of tungsten into lead, as the velocity is increased well above the critical velocity associated with the projectile fragmentation penetration will increase according to $v_o^{2/3}$.

The data for glass spheres impacting aluminum are especially interesting. The projectile is non-metallic and the data extend to much higher velocities, up to 1.2 $\text{cm}/\mu \text{ sec}$. Even at the higher velocities, however, the penetration is increasing with increased velocity at a rate greater than $v_o^{2/3}$. The threshold velocity for energy scaling, $v_o^* > 1.2$, is much higher than v_o^* that required for the aluminum and steel projectile data. This is a result of the extremely small dimensions of the glass spheres, $D_s = .005 \text{ cm}$ as opposed to values of $D_s = .3 \text{ to } .6 \text{ cm}$ for the bulk of the metal-metal data. The effect of size on v_o^* was predicted in an earlier report [2] on the basis of the visco-plastic model of the cratering process. As the velocity of the spheres is further increased the threshold velocity for energy scaling will be attained.

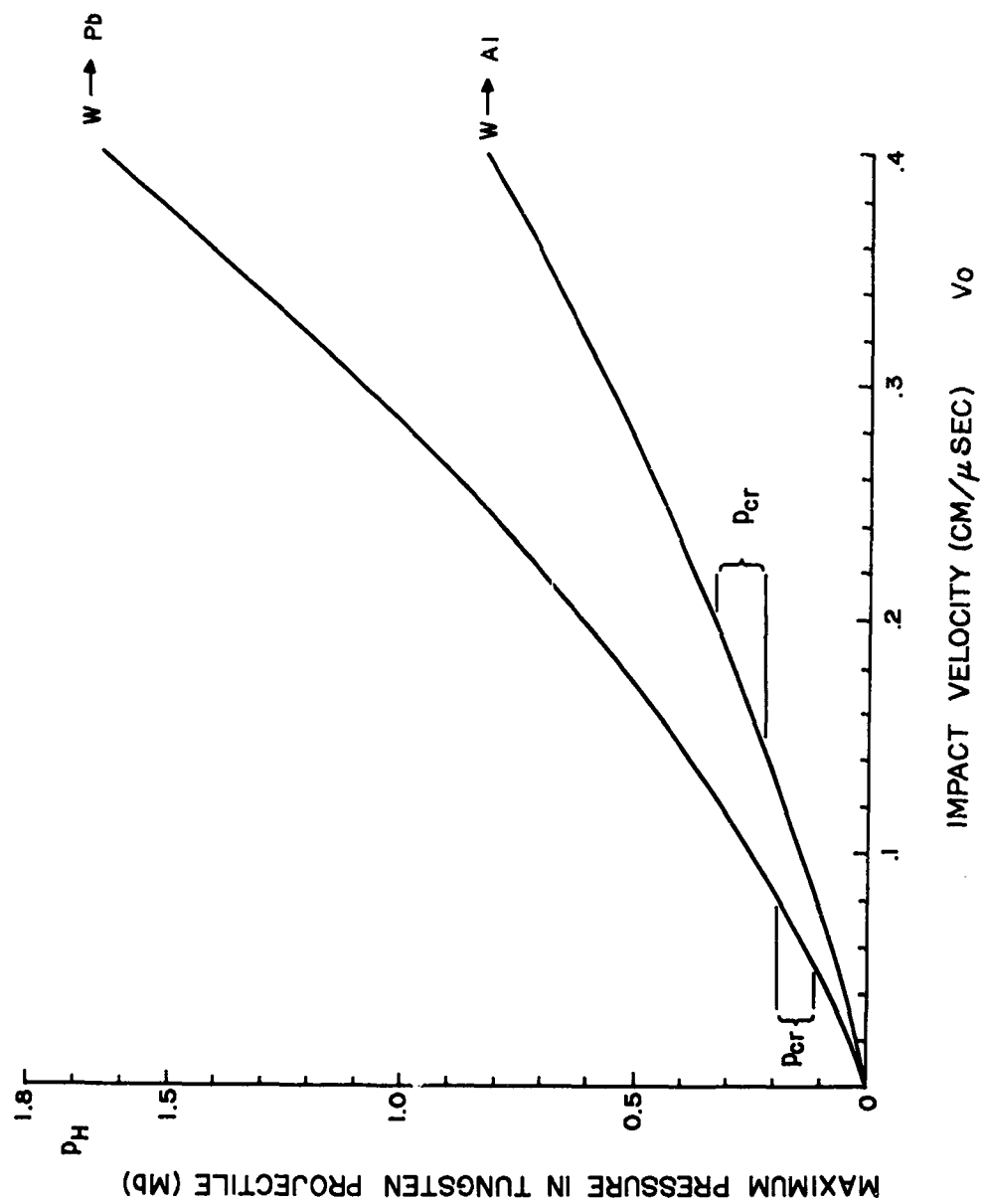


Figure 7. Maximum pressures produced in tungsten projectile impacting lead and aluminum targets at indicated velocities.

SECTION VI

CONCLUSIONS

An analytical method has been applied to determine the peak shock pressures experienced by dissimilar materials subjected to hypervelocity impact. The attenuation of the peak pressures with distance below the target surface is calculated for equi-mass aluminum, iron, copper, and lead projectiles impacting an aluminum target at $2.0 \text{ cm}/\mu\text{sec}$. The computed pressure profiles tend to converge at the lower pressure but do not coalesce.

Available experimental data indicate that the proportionality constant C appearing in the penetration formula (1) depends upon the material of the impacting projectile. The mass and velocity of the projectile are apparently not the only considerations. An explanation of the dependence will be sought in terms of the impedance mismatch at the projectile-target interface. Moreover, detailed calculations using PICWICK II will be made for the case of unlike metal impact.

PICWICK II will also be used for detailed studies of meteor bumper systems and for impact by hollow cylindrical projectiles.

REFERENCES

1. Riney, T. D., "Theoretical Hypervelocity Impact Calculations Using the PICWICK Code," First Interim Report, Contract AF 08(635)-3781, June 1963-December 1963, (ATL-TDR-64-8).
2. Riney, T. D. & Heyda, J. F., "Hypervelocity Impact and Their Correlation with Experiment," Second Interim Report, Contract AF 08(635) 3781, December 1963-June, 1964. Also published as General Electric TIS R64SD64. Also published by Det 4 as ATL-TR-64-64.
3. Heyda, J. F. & Riney, T. D., "Peak Axial Pressures in Semi-Infinite Media Under Hypervelocity Impact," Presented at Seventh Hypervelocity Impact Symposium and published as General Electric TIS R64SD87, November 1964.
4. Heyda, J. F. & Riney, T. D., Report in preparation under NASA Contract NAS 3-4176.
5. Walsh, J. M., Johnson, W. E., Dienes, J. K., Tillotson, J. H., and Yates, D. R., "Summary Report on the Theory of High Speed Impact", General Atomics Report GA-5119 (March 31, 1964).
6. Collins, R. D. & Kinard, W. H., "The Dependency of Penetration on the Momentum per Unit Area of the Impacting Projectile and the Resistance of Materials to Penetration, NASA TN D-238, May, 1960.
7. Maiden, C. J., Gehring, & McMillan, A. R., "Investigation of Fundamental Mechanisms of Damage to Thin Targets by Hypervelocity Projectiles," General Motors Report TR63-225, September 1963.
8. Bruce, E. P., Unpublished data obtained at AEDC.
9. Kincke, J. H., "An Experimental Study of Crater Formation in Metallic Targets," Proc. Fourth Hypervelocity Impact Symposium, Vol. I, 1960.
10. Atkins, W. W., "Hypervelocity Penetration Studies," Proc. Fourth Hypervelocity Impact Symposium, Vol. I. 1960.
11. Rosener, F. C. & Scully, C. N., "Investigation of Structural Implications of Meteoroid Impact," Air Force Flight Dynamics Laboratory Report No. FDL TDR 64-96, July 1964.
12. Charters, A. C., "High Speed Impact," Scientific American, October, Vol. 203, No. 4, October 1960.

INITIAL DISTRIBUTION

1 DOD (DIAAP-1K2)	1 Univ of Chicago (Lib)
1 Hq USAF (AFTAC)	2 Franklin Institute of
1 Hq USAF (AFCIN-3K2)	the State of Penn
2 Hq USAF (AFRDC)	2 SSD (SSTRG/LC W Levin)
1 Hq USAF (AFRAE-E, L/C Hicks)	1 Calif Inst of Tech, Jet
1 Hq USAF (AFTST-EL, Maj Myers)	Propulsion Lab
1 USAF (AFRST-PM/ME, Maj Geiseman)	2 John Hopkins Univ
1 Hq USAF (AFXPDK-NI)	(Applied Rsch Lab)
1 AFSC (SCRWA)	1 OAR (RROSA/Maj Davis)
1 AFSC (SCTA, Mr R Fiek)	1 OAR (RROSA/Maj Metcher)
2 Col Brassfield)	20 DDC
1 AFFDL (FDTS) Mr Parmley	3 Lewis Rsch Ctr
2 ASD (ASAD-Lib)	2 Dir, IDA/Wpns Sys Eval Gp
1 ASD (ASRNGW, Don Lewis)	1 Dir, USAF PROJ RAND
2 AFSWC (Tech Info Div)	(Tech Lib)
1 AFCRL (CRQST-2)	3 Army Materiel Command
1 AFOSR	Rsch Directorate (MCR)
1 AFOSR (SRHP, Dr M M Slawsky)	2 Picatinny Arsenal
1 AFOSR (SRHP, Dr J F Masi)	(SMUPA-DW6)
1 AFOSR (Dr A G Horney)	1 Aberdeen Proving Ground
1 AFOSR (SRHP, Dr R Reed)	(Dr Eichelberger)
1 AFOSR (Dr M A Cook)	1 Aberdeen Proving Ground
1 OOAMA (OOYD)	(J Kineke)
1 NASA	1 Aberdeen Proving Ground
1 NASA (Ofc of Adv Rsch)	(F E Allison)
2 NASA (Tech Lib)	1 Redstone Scientific Info Ctr
1 NASA, Rsch Ctr (W H Kinard)	1 Frankford Arsenal (Lib)
1 NASA, Rsch Ctr (J Stack)	1 Frankford (Pitman-Dunn Lab)
4 NASA, Ames Rsch Ctr (Tech Lib)	2 Springfield Armory
1 Marshall Space Flight Center	(R&D Div)
(W D Murphree)	2 Watertown Arsenal
1 Marshall Space Flight Center	1 Rock Island Arsenal
Adv Rsch Proj Lab (Dr W Johnson)	1 Army Engr Rsch and Dev Lab
1 Adv Rsch Proj Agency (Dr C Bates)	(Tech Doc Ctr)
1 Dir of Def Rsch & Engr (Tech Lib)	1 Dir of Spec Wpns Div
2 Dir of Def Rsch & Engr (Dr R M Yates)	(C. I. Peterson)
2 ARO Scientific Info Br)	1 Army Rsch Ofc - Durham
1 Armour rsch Foundation	(Dr A S Galbraith)
(Mr G H Strohmeir)	4 Bureau of Naval Weapons
1 Aberdeen Proving Ground	(R-12)
(Tech Lib)	4 Bureau of Naval Weapons (RM)
1 White Sands Missile Range	1 US Naval Rsch Lab
	(Code 130/Mr W W Atkins)

2	US Naval Ord Test Stn (Mr L Cosner)	1	U.S.Army, Edgewood Arsenal (Operations Research Gp)
2	USNaval Ord Test Stn (Tech Lib)	1	U.S.Naval Weapons Evaluation Facility (WEVS-1)
2	US Naval Ord Lab (Tech Lib)	1	Wright-Patterson AFB, Ohio (SEPI)
2	US Naval Wpns Lab (Tech Lib)		
1	US Naval Wpns Lab (Dr Soper)		
1	AFMTC (MTBAT)		
4	TAC (DORQ)		
6	General Electric Company		

APGC

4	PGBPS-4
3	PGEH
1	PGOW

RTD Det #4

2	ATWR
1	ATWW
1	ATTR
1	ATB
20	ATBT

UNCLASSIFIED

Security Classification

DOCUMENT CONTROL DATA - R&D		
<small>(Security classification of title, body of abstract and indexing annotation must be entered when the overall report is classified.)</small>		
1 ORIGINATING ACTIVITY (Corporate author) Space Sciences Laboratory, General Electric Co., King of Prussia, Penna.		2a REPORT SECURITY CLASSIFICATION None 2b GROUP
3 REPORT TITLE Attenuation of Shocks Produced by Unlike Metal Impact		
4 DESCRIPTIVE NOTES (Type of report and inclusive dates) Interim Report (24 June 1964 - 31 December 1964)		
5 AUTHOR(S) (Last name, first name, initial) Heyda, J. F. Riney, T. D.		
6 REPORT DATE 29 January 1965	7a TOTAL NO OF PAGES 25	7b NO OF REFS 12
8c. CONTRACT OR GRANT NO. AF 08(635)-3781 b. PROJECT NO. 7234 c. d.	9a ORIGINATOR'S REPORT NUMBER(S) None 9b. OTHER REPORT NO(S) (Any other numbers that may be assigned this report) ATL-TK-65-26	
10 AVAILABILITY/LIMITATION NOTICES Qualified requesters may obtain copies of this report from Defense Documentation Center.		
11. SUPPLEMENTARY NOTES		12. SPONSORING MILITARY ACTIVITY Terminal Ballistics Branch, Det. 4, Research and Technology Division, Eglin Air Force Base, Florida.
13. ABSTRACT An analytical model is presented for determining the peak axial pressure generated at various depths in the target when impacted at hypervelocity by a projectile of similar or dissimilar material. Detailed calculations are given for impact of aluminum, iron, lead and copper into aluminum targets. Available experimental data for impact into aluminum targets are discussed in terms of the theory.		

DD FORM 1 JAN 64 1473

UNCLASSIFIED

Security Classification

UNCLASSIFIED
Security Classification

14. KEY WORDS	LINK A		LINK B		LINK C	
	ROLE	WT	ROLE	WT	ROLE	WT
Impact shock Hypervelocity impact Shock waves in solids Dissimilar metal impact						
INSTRUCTIONS						
<div style="display: flex; justify-content: space-between;"> <div style="width: 48%;"> <p>1. ORIGINATING ACTIVITY: Enter the name and address of the contractor, subcontractor, grantee, Department of Defense activity or other organization (<i>corporate author</i>) issuing the report.</p> <p>2a. REPORT SECURITY CLASSIFICATION: Enter the overall security classification of the report. Indicate whether "Restricted Data" is included. Marking is to be in accordance with appropriate security regulations.</p> <p>2b. GROUP: Automatic downgrading is specified in DoD Directive S200.10 and Armed Forces Industrial Manual. Enter the group number. Also, when applicable, show that optional markings have been used for Group 3 and Group 4 as authorized.</p> <p>3. REPORT TITLE: Enter the complete report title in all capital letters. Titles in all cases should be unclassified. If a meaningful title cannot be selected without classification, show title classification in all capitals in parenthesis immediately following the title.</p> <p>4. DESCRIPTIVE NOTES: If appropriate, enter the type of report, e.g., interim, progress, summary, annual, or final. Give the inclusive dates when a specific reporting period is covered.</p> <p>5. AUTHOR(S): Enter the name(s) of author(s) as shown on or in the report. Enter last name, first name, middle initial. If military, show rank and branch of service. The name of the principal author is an absolute minimum requirement.</p> <p>6. REPORT DATE: Enter the date of the report as day, month, year, or month, year. If more than one date appears on the report, use date of publication.</p> <p>7a. TOTAL NUMBER OF PAGES: The total page count should follow normal pagination procedures, i.e., enter the number of pages containing information.</p> <p>7b. NUMBER OF REFERENCES: Enter the total number of references cited in the report.</p> <p>8a. CONTRACT OR GRANT NUMBER: If appropriate, enter the applicable number of the contract or grant under which the report was written.</p> <p>8b, 8c, & 8d. PROJECT NUMBER: Enter the appropriate military department identification, such as project number, subproject number, system numbers, task number, etc.</p> <p>9a. ORIGINATOR'S REPORT NUMBER(S): Enter the official report number by which the document will be identified and controlled by the originating activity. This number must be unique to this report.</p> <p>9b. OTHER REPORT NUMBER(S): If the report has been assigned any other report numbers (<i>either by the originator or by the sponsor</i>), also enter this number(s).</p> </div> <div style="width: 48%;"> <p>10. AVAILABILITY/LIMITATION NOTICES: Enter any limitations on further dissemination of the report, other than those imposed by security classification, using standard statements such as:</p> <p>(1) "Qualified requesters may obtain copies of this report from DDC."</p> <p>(2) "Foreign announcement and dissemination of this report by DDC is not authorized."</p> <p>(3) "U. S. Government agencies may obtain copies of this report directly from DDC. Other qualified DDC users shall request through _____."</p> <p>(4) "U. S. military agencies may obtain copies of this report directly from DDC. Other qualified users shall request through _____."</p> <p>(5) "All distribution of this report is controlled. Qualified DDC users shall request through _____."</p> <p>If the report has been furnished to the Office of Technical Services, Department of Commerce, for sale to the public, indicate this fact and enter the price, if known.</p> <p>11. SUPPLEMENTARY NOTES: Use for additional explanatory notes.</p> <p>12. SPONSORING MILITARY ACTIVITY: Enter the name of the departmental project office or laboratory sponsoring (<i>paying for</i>) the research and development. Include address.</p> <p>13. ABSTRACT: Enter an abstract giving a brief and factual summary of the document indicative of the report, even though it may also appear elsewhere in the body of the technical report. If additional space is required, a continuation sheet shall be attached.</p> <p>It is highly desirable that the abstract of classified reports be unclassified. Each paragraph of the abstract shall end with an indication of the military security classification of the information in the paragraph, represented as (TS), (S), (C), or (U).</p> <p>There is no limitation on the length of the abstract. However, the suggested length is from 150 to 225 words.</p> <p>14. KEY WORDS: Key words are technically meaningful terms or short phrases that characterize a report and may be used as index entries for cataloging the report. Key words must be selected so that no security classification is required. Identifiers, such as equipment model designation, trade name, military project code name, geographic location, may be used as key words but will be followed by an indication of technical context. The assignment of links, rules, and weights is optional.</p> </div> </div>						

UNCLASSIFIED
Security Classification

UNCLASSIFIED

UNCLASSIFIED